Ratner, L., Wiegand, R. C., Farrell, P. J., Sen, G. C., Cabrer, B., & Lengyel, P. (1978) *Biochem. Biophys. Res. Commun. 81*, 947-954.
Sawai, H., & Ohno, M. (1981a) *Chem. Pharm. Bull. 29*, 2231-2245.
Sawai, H., & Ohno, M. (1981b) *Bull. Chem. Soc. Jpn. 54*, 2759-2762.
Sawai, H., & Shinomiya, T. (1982) *J. Biochem. (Tokyo) 92*, 1723-1730.
Sawai, H., Shibata, T., & Ohno, M. (1981) *Tetrahedron 37*, 481-485.
Sawai, H., Imai, J., Lesiak, K., Johnston, M. I., & Torrence, P. F. (1983) *J. Biol. Chem. 258*, 1671-1677.
Shinomiya, T., Funayama-Machida, C., & Uchida, T. (1978) *J. Biochem. (Tokyo) 84*, 1447-1451.
Silverman, R. H., Cayley, P. J., Knight, M., Gilbert, C. S., & Kerr, I. M. (1982) *Eur. J. Biochem. 124*, 131-138.
Stark, G. R., Dower, W. J., Schimke, R. T., Brown, R. E., & Kerr, I. M. (1979) *Nature (London) 278*, 471-473.
Stollar, B. D. (1975) *CRC Crit. Rev. Biochem. 3*, 45-69.
Torrence, P. F., Imai, J., & Johnston, M. I. (1981a) *Proc. Natl. Acad. Sci. U.S.A. 78*, 5993-5997.
Torrence, P. F., Johnston, M. I., Epstein, D. A., Jacobsen, H., & Friedman, R. M. (1981b) *FEBS Lett. 130*, 291-296.
Ts'o, P. O. P., Kondo, N. S., Schweizer, M. P., & Hollis, D. P. (1969) *Biochemistry 8*, 997-1029.
Wallace, S. S., Erlanger, B. F., & Beiser, S. M. (1971) *Biochemistry 10*, 679-683.
Williams, B. R. G., & Kerr, I. M. (1978) *Nature (London) 276*, 88-89.
Williams, B. R. G., Kerr, I. M., Gilbert, C. S., White, C. N., & Ball, L. A. (1978) *Eur. J. Biochem. 92*, 455-462.
Williams, B. R. G., Golgher, R. R., Brown, R. E., Gilbert, C. S., & Kerr, I. M. (1979) *Nature (London) 282*, 582-586.
Williams, C. A., & Chase, M. W. (1971) *Methods Immunol. Immunochem. 3*, 1-58.
Wreschner, D. H., James, T. C., Silverman, R. H., & Kerr, I. M. (1981a) *Nucleic Acids Res. 9*, 1571-1581.
Wreschner, D. H., McCauley, J. W., Skehel, J. J., & Kerr, I. M. (1981b) *Nature (London) 289*, 414-417.

Quantitative Analysis of Resonance Raman Spectra of Purple Membrane from *Halobacterium halobium*: L550 Intermediate†

Pramod V. Argade‡ and Kenneth J. Rothschild*

ABSTRACT: The bacteriorhodopsin photocycle consists of a series of intermediates, each characterized by a different visible absorption. We have examined one of these intermediates, L550, by *quantitatively* analyzing the resonance Raman spectra of purple membrane recorded under different conditions. A rotating cell was used to control the contribution of the early intermediates in the resonance Raman spectra. These spectra were then fitted to a superposition of Voigtian line shapes to obtain the position, width, and integrated intensity of each band. We find evidence for the appearance within 5 μs of two bands at 1539 and 1551 cm^{-1}. By correlating the intensity changes in these bands with the protonated Schiff base band, we are able to establish that the intermediates giving rise to them are protonated. It is thus concluded that M412 is the first deprotonated intermediate in the bateriorhodopsin photocycle. Because the ratio of the integrated intensity of 1539- and 1551-cm^{-1} bands remains constant for various exposure times and laser power, the possibility is discussed that they both arise from the L550 intermediate rather than from L550 and a second "X" intermediate as previously proposed. In addition, it is concluded that a conformational change in the chromophore has occurred in L550 relative to that in the light-adapted bR570. A possible linear relation between C=N stretching frequency and wavelength maximum for visible absorption is discussed.

Much interest has focused on bacteriorhodpsin, the light-transducing proton pump of the purple membrane (PM)[1] in *Halobacterium halobium* [for a review see Stoeckenius et al. (1979)]. In contrast to other membrane transport proteins, considerable information is available about bacteriorhodopsin including its amino acid sequence (Ovchinnikov et al., 1979; Khorana et al., 1979) and secondary structure (Henderson & Unwin, 1975; Engelman et al., 1980). However, the basic mechanism of bacteriorhodopsin proton translocation and energy transduction still remains unelucidated.

In order for further progress to be made, it will be necessary to elucidate in detail the molecular changes occurring in both the protein, bacterioopsin, and the chromophore, retinal, subsequent to light absorption. Resonance Raman spectroscopy (RRS) offers a selective method of probing the chromophore during the bacteriorhodopsin proton pump cycle. Information obtained by using this method thus far indicates the following: (i) A linear correlation exists between the C=C stretching frequency of the isoprene chain of the retinylidene chromophore (1500-1570-cm^{-1} range) and the absorption maximum of the spectral intermediates (Heyde et al., 1971; Aton et al., 1977; Doukas et al., 1978). This correlation can be used to identify the presence of different intermediates in the RRS of PM. (ii) The bands at 1642 cm^{-1} in the light-

† From the Department of Physics and Department of Physiology, Boston University, Boston, Massachusetts 02215. *Received December 27, 1982.* This work was supported by National Institutes of Health Grants EY02142 and EY01996, National Science Foundation Grant 80-11509, and Established Investigatorship Award from the American Heart Association to K.J.R.
‡ Present address: Bell Laboratories, Murray Hill, NJ 07974.

[1] Abbreviations: BR, bacteriorhodopsin; PM, purple membrane; RRS, resonance Raman spectrum.

0006-2960/83/0422-3460$01.50/0

adapted bR570 state and 1622 cm^{-1} in the M412 intermediate of the photocycle have been identified as due to the protonated and deprotonated Schiff base linkage, respectively (Lewis et al., 1974; Marcus & Lewis, 1978; Stockburger et al., 1979; Argade et al., 1981). However, it is not clear at what stage the deprotonation of the Schiff base occurs prior to the formation of M412. (iii) The structurally sensitive "fingerprint" region (1100–1450 cm^{-1}) can give information about the conformation of the chromophore mainly by comparison with model compounds (Aton et al., 1977; Terner et al., 1977; Marcus & Lewis, 1978) and has been used, for example, to provide evidence that bR570 has an all-trans chromophore and that of the K and M412 intermediates is in a 13-cis configuration (Braiman & Mathies, 1980, 1982). (iv) The attachment site of the retinal chromophore to lysine can be probed by introducing selective isotopic labeling in the protein (Rothschild et al., 1982).

It has been the goal of several groups to systematically determine the RRS of all the intermediates in the bacteriorhodopsin photocycle. However, a major difficulty in the analysis of RRS of PM is the presence of overlapping bands contributed from several different intermediates present under steady-state conditions. Kinetic RRS methods such as rapid flow techniques partially alleviate this problem by reducing the number of contributing intermediates in the spectrum (Mathies et al., 1976; Callender et al., 1976; Aton et al., 1977; Marcus & Lewis, 1977, 1978; Terner et al., 1979a; Stockburger et al., 1979). However, it has proven difficult to obtain a spectrum of an intermediate other than bR570 and M412 as indicated by the lack of agreement for the reported spectra of other intermediates. Part of this problem stems from the method of subtracting spectra (Terner et al., 1979a–c; Stockburger et al., 1979; Narva et al., 1981). This method has three major drawbacks: (i) There is no guide for the proportion in which the spectra are to be subtracted, and rather ad hoc assumptions have to be made. (ii) When two spectra are subtracted, the noise level increases, and hence the signal to noise ratio decreases. (iii) The subtracting procedure does not compare the changes in the integrated intensity of bands but compares the intensity changes point by point.

In this paper, we describe the utilization of a resonance Raman kinetic method in conjunction with curve fitting of spectra to resolve the contributions from overlapping bands. This method allows us to analyze the spectra quantitatively. The integrated intensity, half-width, and frequency of bands due to intermediates can be accurately determined. When the contribution of the intermediates to the spectrum is varied and changes of integrated intensity of bands are correlated it is possible to determine the state of protonation of different intermediates. We show in this paper that L550 has a protonated Schiff base; thus the deprotonation of BR Schiff base occurs between L550 and M412.

Materials and Methods

Halobacteria were grown, and PM was isolated by using the method of Becher & Cassim (1975). A strain of halobacteria S_1 was used, which contained an enriched amount of PM and no carotenoids [as determined by the bands at 1515 and 1157 cm^{-1} in RRS (Rimai et al., 1970)]. PM was extensively washed in double-distilled water and dialyzed for 24 h in order to remove sucrose and other contaminants.

Resonance Raman spectra of PM suspension were recorded by using a "home-built" rotating sample cell (Stockburger et al., 1979; Argade & Rothschild, 1982). The radius of the cell, r, was 2.32 cm, which was also the separation of the laser beam from the axis of rotation of the cell. The speed of rotation of the cell was regulated within 5% error by using a home-built photoelectric feedback system (Argade & Rothschild, 1982) which measured also the frequency of rotation, f. The diameter of the laser beam, d, at the sample was 40 μm. Hence, the sample exposure time was

$$t = d/(2\pi fr)$$

and time between the exposures was

$$T = 1/f$$

Since a 100-μm input slit, s, of the double monochromator was adjusted at the center of the 5-fold magnified image of scattered laser, the effective sample exposure time was

$$t_e = \frac{d}{2\pi fr}\,\frac{(5d/2 + s/2)}{5d}$$

For all the spectra recorded, T was more than 5 times the cycle time for bacteriorhodopsin. Hence, a complete rotation of the cell allowed sufficient time for almost all the bacteriorhodopsin to relax back to the bR570 state before it was again exposed to the laser beam. To record a spectrum of bR_{570}, we used f = 40 Hz (t_e = 5.2 μs, T = 25 ms) and 5 mW of power at the sample using 514.5-nm laser line (photoreaction rate constant $I_0 = 4.17 \times 10^4$ s^{-1}; Stockburger et al., 1979). Under these conditions the resultant spectrum had more than 97% contribution from bR570. In order to obtain a varying contribution from intermediates preceding M412, the speed of rotation of the cell was varied in the range f = 40–10 Hz (t_e = 5.1–24 μs), and the power was varied between 10 and 100 mW ($I_0 = 4.17 \times 10^4$ to 4.17×10^5 s^{-1}). The effective sample exposure time under these conditions was sufficient to allow contributions to build up from M412 and the intermediates preceding it. Spectra were also recorded when the same setup with the 488.0-nm laser line was used.

Raman spectra were recorded on a Ramalog IV Raman spectrometer consisting of Spex Model 1401 double monochromator and a thermoelectrically cooled (Model TE-104, Products for Research, Inc.) photomultiplier tube (RCA C31034) operated in the photon counting mode. The spectrometer was interfaced to a Nic-1180 data system (Nicolet Instrument Corp., Inc.) to acquire data on-line. The exciting source was a 4-W argon ion laser (Spectra-Physics, Model 164). The spectrometer was calibrated by using 218- and 314-cm^{-1} bands of carbon tetrachloride. The PM spectra were multiply scanned in the range 800–1700 cm^{-1} to increase the signal to noise ratio and consisted of 1024 points. Spectral resolution was 2 cm^{-1}. The data stored in Nic-1180 were transferred to an IBM 370/168 computer,[2] where it was analyzed and plotted on a Calcomp plotter (Model 763).

Analysis of Data

We assumed a Lorentzian line shape for the Raman bands. At small spectrometer slit width, the "instrument function" is a Gaussian.[3] The line shape recorded by the spectrometer is the convolution of the Raman line shape and the instrument function and in this case is called a Voigtian line shape (Armstrong, 1967). We found by computer simulation that the Voigtian line shape differs significantly from a Lorentzian when the Lorentzian bandwidth is smaller than 5 times the spectral resolution, which is 2 cm^{-1} in our case. Since some

[2] For an Assembly language listing of interprocessor communications program ADITI2, see Argade (1982).

[3] The instrument function was obtained by recording the scattering of the laser beam from air. With a 100-μm input slit of the double monochromator, the instrument function was found to be a Gaussian with a half-width of 2 cm^{-1}.

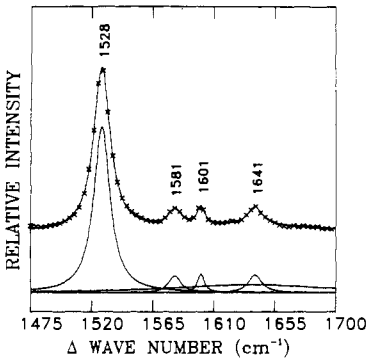

FIGURE 1: A spectrum of bR570 recorded with a rotating cell using a 514.5-nm laser line. Effective sample exposure time t_e = 5 μs and laser power = 5 mW. The spectrum was recorded in the range 800–1700 cm^{-1} and consisted of 1024 data points. It was fitted in the range 1475–1700 which consisted of 256 data points. Every fourth data point is shown for clarity by (×). The fitted spectrum and the constituent band are also shown. The reduced χ^2 value for this fitting was 1.56. During the fitting procedure the position and width of the band due to water were fixed at 1635 and 140 cm^{-1}, respectively.

bands in the Raman spectrum of PM have a bandwidth of 7 cm^{-1}, the effect of instrument function on the band shape is significant. Hence, we fitted the Raman spectra of PM recorded under various conditions as described above to superposition of Voigtians.

All the PM spectra were fitted in the range 1475–1700 cm^{-1} which consisted of 256 data points. This range is of particular interest because it contains bands due to the C=C stretching vibration which are indicative of the presence of various intermediates (Doukas et al., 1978) and also has the bands due to the Schiff base linkage. For curve fitting, the method of least squares by linearization of the fitting function was implemented using Marquard's algorithm. This procedure is described in detail by Sindius (1973) and Bevington (1969). The curve-fitting program is designed for fitting a maximum of 10 overlapping bands. For each band the fitting parameters are position, bandwidth (the full width at half-maximum), and integrated intensity. Since the base line of the spectrum is in general flat, two base-line parameters, a constant and the slope, were sufficient for the base-line fitting. An initial guess of all the parameters was provided to the program which calculated the optimum parameters along with the standard deviation in the parameters. These parameters were used in turn as initial guesses for the next iteration. This procedure was terminated when an acceptable χ^2 value was obtained. During the fitting procedure, some parameters could be held fixed at a given value. Prior to the curve fitting, each spectrum was smoothed once by averaging over one channel on both sides (i.e., three points smooth) (Bevington, 1969).

The curve fitting procedure has to be used very carefully, since it can lead to erroneous conclusions. We verified that when physically acceptable fitted parameters were obtained (i.e., all the band parameters were positive), they were independent of the initial guess. Consistency of the band position and the bandwidth was verified by comparing parameters for various spectra. The "goodness" of the fitted parameters was determined by the reduced χ^2 value, whose expected value is 1. In general, we obtained reduced χ^2 values close to 1.

In all the spectra of suspensions of PM in water, a broad band due to water near 1635 cm^{-1} is evident (Terner et al., 1979a). By use of a similar curve-fitting procedure for distilled water, this band was found to be at 1635 cm^{-1} with a bandwidth of 140 cm^{-1}. Since the protonated Schiff base vibration for PM also lies near 1635 cm^{-1}, the position and width of the band due to water were kept fixed at 1635 and 140 cm^{-1}, respectively, while fitting the spectrum of PM.

Table I: Fitted Parameters for the Spectrum of bR570[a]

position (cm^{-1})	width (cm^{-1})	intensity
1527.6 ± 0.0[b]	14.6 ± 0.3	100 ± 0.6
1581.2 ± 0.3	12.3 ± 0.7	8.7 ± 0.5
1600.5 ± 0.3	7.1 ± 0.5	5.2 ± 0.5
1640.5 ± 0.3	13.4 ± 0.8	10.0 ± 0.7

[a] The mean values obtained for the five spectra recorded under identical conditions are shown along with the standard deviations (these are not the standard deviations in the mean). This table shows that consistent parameters can be obtained by the curve-fitting procedure. [b] The absolute determination of the peak position is limited by the calibration of the spectrometer.

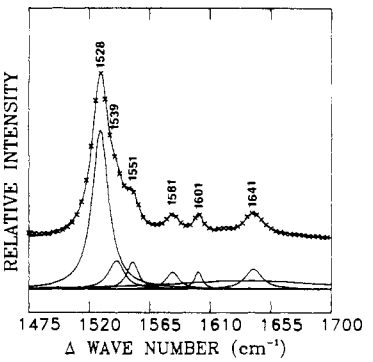

FIGURE 2: Spectrum recorded with rotating cell using effective sample exposure time t_e = 17 μs, time between exposures T = 83 ms, and laser power = 100 mW. The photoreaction rate constant was I_0^0 = 4.17 × 10^5 s^{-1}. It is evident from the absence of a band at 1567 cm^{-1} that there is no contribution from M412 intermediate. The fitted spectrum and constituent bands are also shown. Since the width of the 1528-cm^{-1} band must be characteristic of the bR_{570} intermediate and is not expected to change under the conditions of this, its half-width was held fixed at 14.6 cm^{-1} (cf. Table I) while fitting. Also the position and width of water were fixed at 1635 and 140 cm^{-1}, respectively. The χ^2 value for the fit was 0.61.

Results and Discussion

Figure 1 shows a RRS of bR570. A single symmetric band at 1528 cm^{-1} shows that the contribution to the spectrum is predominantly from bR570. Figure 1 also shows the fitted spectrum and constituent bands. The 1528-cm^{-1} band is assigned to the C=C stretching vibration of bR570 (Lewis et al., 1974; Aton et al., 1977). The 1641-cm^{-1} band is assigned to the protonated Schiff base vibration (Lewis et al., 1974). The origin of the 1581- and 1601-cm^{-1} bands is not clearly understood but may also arise from individual C=C stretches. Table I lists the position, half-width, and integrated intensity for all the bands in Figure 1. Five spectra were recorded under identical conditions, and the parameters listed represent the mean values obtained by fitting them. The standard deviations in the parameters are also shown. The curve-fitting program also calculated the standard deviations in the fitted parameters for each spectrum. They were in excellent agreement with the standard deviation in the parameters calculated for the five spectra.

A spectrum resulting from slowing the speed of rotation of the cell and increasing the power is shown in Figure 2. The sample exposure time (t_e = 17 μs) and time between exposures (T = 83 ms) were such that only intermediates up to M412 contributed to the spectrum. This is evident since no detectable contribution from the M412 intermediate appears in the spectrum as determined by the absence of the characteristic band at 1567 cm^{-1} (Lewis et al., 1974; Aton et al., 1977). Two shoulders at 1539 and 1551 cm^{-1} are evident. The constituent

Table II: Fitted Parameters for the Spectra Having Contributions from Intermediates up to but Not Including M412[a]

position (cm^{-1})	width (cm^{-1})	intensity
1527.6 ± 0.0	14.6	100 ± 1.1
1539.3 ± 0.4	12.8 ± 1.7	17.6 ± 2.3
1551.3 ± 0.3	11.5 ± 0.7	12.5 ± 1.3
1581.3 ± 0.2	11.7 ± 1.2	8.9 ± 0.4
1600.6 ± 0.2	7.5 ± 0.6	5.5 ± 0.4
1641.1 ± 0.3	15.5 ± 0.7	13.9 ± 0.9

[a] The position and half-width shown are the mean values calculated for the 12 spectra recorded by using rotating cell with 514.5-nm laser line at various power and sample exposure time. The standard deviations are also shown (these are not the standard deviation in the mean). Since the relative intensities of various bands for the 12 spectra differed, the intensities shown are those for the spectrum in Figure 2. The standard deviations in the intensity were calculated by the program. The consistency in the position and half-width of the bands at 1539 and 1551 cm^{-1} strongly indicates their existence in the Raman spectrum.

bands obtained by curve fitting are shown in Figure 2.

In order to verify the existence of bands at 1539 and 1551 cm^{-1} in the spectrum, we recorded 12 spectra at various combinations of incident laser power (10–100 mW) and sample exposure times (5–17 μs). In all of these spectra, there was no detectable contribution from M412. All the spectra thus obtained were fitted by using the same procedure as applied in Figure 2. When only six bands were assumed to exist, no satisfactorily fitted parameters were obtained, and the position and half-width of the band obtained around 1548 cm^{-1} were not consistent for all 12 spectra. In contrast, when seven bands were assumed to contribute, the curve-fitting program resolved bands at 1539 and 1551 cm^{-1} whose position and width were consistent for all 12 spectra (cf. Table II), hence strongly implying the existence of these bands in the spectrum. Table III summarizes the intensities at 1539, 1551, and 1641 cm^{-1} for the 12 spectra.

Although the band at 1551 cm^{-1} has been reported before, the existence of the band at 1539 cm^{-1} has been disputed. Using kinetic resonance Raman spectroscopy, Marcus & Lewis (1978) observed a band at 1537 cm^{-1} which they assigned to the C=C stretching vibration of the L550 intermediate. They also found evidence that the L550 is protonated. On the basis of a second band at 1552 cm^{-1}, they proposed the existence of a *deprotonated* intermediate, "X", absorbing maximally between 460 and 485 nm and appearing after L550. In contrast Campion et al. (1977) and Terner et al. (1977) did not report a band at 1537 cm^{-1} and assigned the 1551-cm^{-1} band to the L550 intermediate. In addition they first proposed that the L550 is deprotonated (Terner & El-Sayed, 1978) but later found evidence for protonation (Terner et al., 1979a).

In order to further characterize the origin of bands at 1539 and 1551 cm^{-1}, we studied the correlation in the intensity of these bands with the protonated Schiff base band at 1641 cm^{-1}. In all of the 12 spectra described above, we observed no evidence of a deprotonated Schiff base vibration at 1620 cm^{-1}. In order to take the contribution of the bR570 to the protonated Schiff base into account, we normalized all 12 spectra such that the 1528-cm^{-1} band had a unit intensity in each case (cf. Table III). Thus, the intensity *changes* in the 1641-cm^{-1} band were solely due to the contribution from the intermediate(s) giving rise to the 1539- and 1551-cm^{-1} bands.

Figure 3 shows the intensity of the 1539-cm^{-1} band vs. the 1641-cm^{-1} band when the 1528-cm^{-1} band was normalized to one. We find a linear correlation with a slope and x intercept of 4.1 ± 0.35 and 0.10 ± 0.004, respectively. Figure 4 shows the correlation between the 1551-cm^{-1} band and the 1641-cm^{-1} band when the 1528-cm^{-1} band was normalized to one. In this case we also find a linear correlation with a slope and x intercept of 2.83 ± 0.18 and 0.092 ± 0.004, respectively.[4]

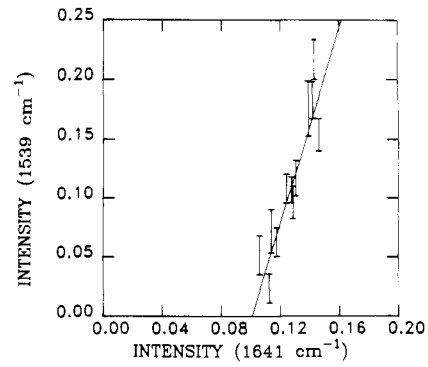

FIGURE 3: Intensity of the 1539-cm^{-1} band is plotted vs. that of the 1641-cm^{-1} band for the 12 spectra obtained by using the rotating cell setup at 514.5-nm laser line. All the spectra were fitted by using an identical procedure, and then the intensity of the 1528-cm^{-1} band was normalized to one. Least-squares fit to a straight line gave estimates of slope and intercept on the x axis of 4.1 ± 0.35 and 0.10 ± 0.004, respectively. The linear correlation coefficient was 0.92.

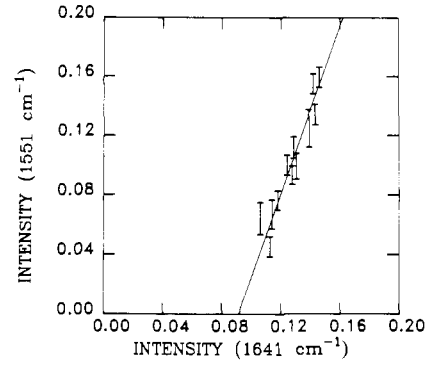

FIGURE 4: Intensity of the 1551-cm^{-1} band is plotted vs. that of the 1641-cm^{-1} band for the 12 spectra described in Figure 3. Least-squares fit to a straight line gave estimates of slope and intercept on the x axis of 2.83 ± 0.18 and 0.09 ± 0.004, respectively. The linear correlation coefficient was 0.95.

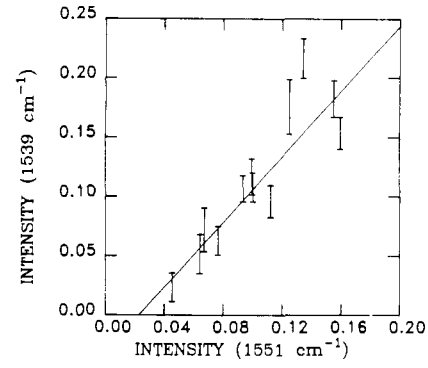

FIGURE 5: Intensity of the 1539-cm^{-1} band is plotted vs. that of the 1551-cm^{-1} band for the 12 spectra described in Figure 4. Least-squares fit to a straight line gave estimates of slope and intercept on the x axis of 1.38 ± 0.12 and 0.04 ± 0.01, respectively. The linear correlation coefficient was 0.9.

The linear correlations obtained in Figures 3 and 4 are possible only if the 1539- and 1551-cm^{-1} bands occur in fixed

[4] It is important to note that the slopes in Figures 3 and 4 correspond to the ratio of the change in the integrated intensity of the C=C stretching band at 1539 and 1551 cm^{-1}, respectively, to that of the protonated Schiff base band. These ratios are smaller than 10 ± 0.7 obtained for the 1528-cm^{-1} band (cf. Table I). The intercept on the x axis in Figures 3 and 4 corresponds to the intensity of the 1641-cm^{-1} band for a unit intensity of the 1528-cm^{-1} band.

Table III: Experimental Conditions and Relative Intensities of 1539-, 1551-, and 1641-cm^{-1} Bands for the 12 Spectra Recorded at 5145-Å Laser Line[a]

laser power (mW)	$I_0 \times 10^{-4}$ (s^{-1})	t_e (μs)	$I_0 t_e$	$I_{1539} \times 10^2$	$I_{1551} \times 10^2$	$I_{1641} \times 10^2$
10	8.3	5.3	0.44	5.2 ± 1.7	6.4 ± 1.1	10.6 ± 0.9
10	8.3	5.3	0.44	7.2 ± 1.9	6.3 ± 0.9	10.7 ± 0.6
30	25	6.1	1.53	2.4 ± 1.2	4.5 ± 0.7	11.3 ± 0.5
30	25	18.7	4.68	6.3 ± 1.2	7.6 ± 0.6	11.8 ± 0.4
70	58	9.8	5.68	10.8 ± 1.3	10.0 ± 0.7	12.4 ± 0.4
70	58	9.8	5.68	10.7 ± 1.1	9.3 ± 0.6	12.8 ± 0.4
70	58	9.8	5.68	9.6 ± 1.4	11.2 ± 0.7	12.9 ± 0.5
100	83	9.8	8.13	11.7 ± 1.6	9.9 ± 0.9	13.1 ± 0.6
70	58	17.2	9.97	18.3 ± 1.6	15.5 ± 0.7	14.2 ± 0.4
70	58	17.2	9.97	21.7 ± 1.8	13.4 ± 0.7	14.3 ± 0.5
70	58	17.2	9.97	15.4 ± 1.4	15.9 ± 0.7	14.6 ± 0.4
100	83	17.2	14.3	17.6 ± 2.3	12.5 ± 1.3	13.9 ± 0.9

[a] All the spectra were normalized such that the 1528-cm^{-1} bands had a unit intensity after fitting. The instrumental error in the measurement of laser power ranges from ±50% at 10 mW to ±20% at 100 mW.

Table IV: Summary of the Results of the Plots Similar to Those in Figures 3–5 Made for the Nine Spectra Recorded at 488 nm Using the Rotating Cell Setup[a]

abscissa (cm^{-1})	ordinate (cm^{-1})	slope	intercept	r
1641	1539	3.26 ± 0.32	0.12 ± 0.004	0.92
1641	1551	3.85 ± 0.26	0.11 ± 0.01	0.86
1551	1539	0.75 ± 0.08	0.04 ± 0.02	0.86

[a] The relative concentration of the intermediates was varied by adjusting the sample exposure time and incident laser power. For all these spectra there was no contribution from M412 intermediate. r, linear correlation coefficient.

proportions. Figure 5 shows the correlation between the integrated intensity of the 1539- and 1551-cm^{-1} bands when the 1528-cm^{-1} band was normalized to one. In this case, as expected, we obtain a linear correlation with slope and intercept, 1.38 ± 0.12 and 0.04 ± 0.01, respectively.[5] Hence, if the 1539- and 1551-cm^{-1} bands arise from two distinct intermediates, their concentrations appear to remain in a fixed ratio under a variety of conditions. Since there is no detectable contribution from a deprotonated Schiff base band at 1620 cm^{-1} in any of these spectra, we conclude that the intermediates which give rise to the 1539- and 1551-cm^{-1} bands are protonated.

We also recorded nine spectra using the rotating cell with various combinations of sample exposure times and incident laser powers at 488 nm. All nine spectra thus obtained were fitted, and plots similar to those in Figures 3–5 were made. The results are summarized in Table IV. It is evident from Table IV that all the linear correlations observed in spectra recorded at 514.5 nm are also observed in those recorded at 488 nm.

L550 Intermediate. It is possible to determine quantitatively the L550 spectrum by utilizing the fact that the curve-fitting procedure determines the contribution of each of the major components of the spectrum. Hence, the need to arbitrarily subtract different amounts of one spectrum from another is eliminated. Parts A and B of Figure 6 show the spectra in Figures 1 and 2, respectively, from 800 to 1700 cm^{-1} with the background obtained from curve-fitting subtracted out. Figure 6C shows the difference of parts A and B after the integrated intensity of the 1528-cm^{-1} band in each speectrum is normalized. This difference should reflect the RRS of L550. It is noted, however, that the band at 1551 cm^{-1} which has previously been associated with the X intermediate cannot be eliminated by using this procedure since as discussed above both 1551 and 1539 cm^{-1} always occur in fixed proportion to each other.

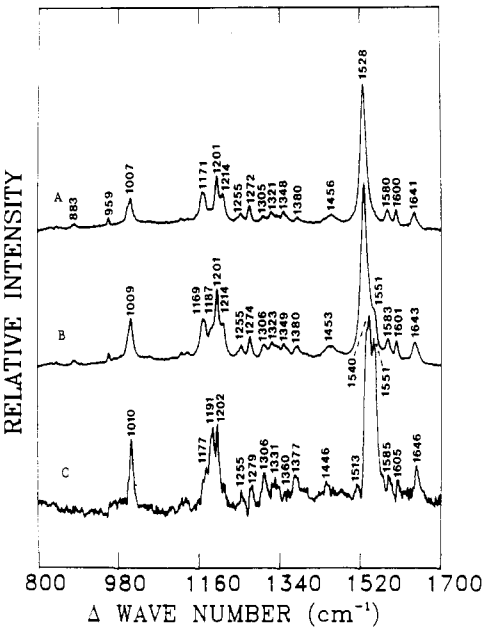

FIGURE 6: (A) Pure spectrum of bR570 shown in Figure 1 but in the range 800–1700 cm^{-1}. The contribution of background and the band due to water at 1635 cm^{-1} obtained from curve fitting were subtracted out. (B) Spectrum shown in Figure 2 but in the range 800–1700 cm^{-1}. The background and band due to water were subtracted out by the similar method. The spectrum was normalized such that the 1528-cm^{-1} band had the same intensity in (A) and (B). (C) Spectrum in (A) was subtracted from that in (B). This spectrum is magnified 4 times for comparison.

The spectrum of L550 shown in Figure 6C is in very good agreement with the spectrum reported by Stockburger et al. (1979) recorded at 5-cm^{-1} resolution. Since the resolution in our case was 2 cm^{-1}, more features are clearly resolved. In particular the 1539- and 1551-cm^{-1} bands are distinct. Furthermore, contrary to previous reports (Marcus & Lewis, 1978; Terner & El-Sayed, 1978) we observe only a protonated Schiff base vibration at 1646 cm^{-1}. It is interesting that this band is shifted 4 cm^{-1} higher than the band in bR570. We also note that Figure 6C does not agree closely with the composite spectrum of L and the photoproduct L′ recorded at −193° (Narva et al., 1981). In particular, under these conditions only

[5] It is noted that the slopes in Figures 3–5 are related to each other. For example, the slope of the line in Figure 3 is predicted to be 3.9 ± 0.4 from the slopes of the curves in Figures 4 and 5 within the limits of error of the actual slope, 4.1 ± 0.4.

a single peak is observed with a frequency at 1533 cm^{-1}. In addition, the figerprint region reported differs considerably from Figure 6C.

From the structurally sensitive fingerprint region some indication of the configuration of the L550 chromophore can be surmised. The chromophore extraction work of Tsuda et al. (1980) indicates that light isomerizes the chromophore from all-trans in bR570 to 13-cis by the time of appearance of the L intermediate. Also, Braiman & Mathies (1980, 1982) have demonstrated that both K and M412 have a 13-cis chromophore. Thus, it is likely that L550, which lies between K and M412 in the photocycle, may also have a 13-cis chromophore. Since our spectrum of L550 has a fingerprint region quite distinct from that of K and M412 (Braiman & Mathies, 1980, 1982), the chromophore is likely to have additional constraints; however, its exact nature cannot be determined from the present work.

A second important feature of the L550 spectrum is the existence of a peak at 1646 cm^{-1} which is 4 cm^{-1} higher than the peak in bR570 assigned to the C=N stretch of the protonated Schiff base. A peak at 1648 cm^{-1} is also reported in the low temperature spectrum of L and L′ (Narva et al., 1981). In contrast, recent studies on the K intermediate by Fourier transform infrared difference spectroscopy (Rothschild & Marrero, 1982) indicate the possibility of a much lower protonated Schiff base frequency at 1610 cm^{-1}. Hence, it appears that while bR570, K, and L550 all contain protonated Schiff bases, the stretching frequency first shifts down and then up relative to bR570. This suggests for the first time that a definite relationship between the C=N stretching frequency and wavelength of maximum absorption in the visible of the intermediate exists. For example, a simple plot of these two parameters for bR570 (570 nm, 1641 cm^{-1}), L550 (550 nm, 1646 cm^{-1}) and K (630 nm, 1610 cm^{-1}) reveals a linear relation (K. J. Rothschild, unpublished results). Such a relation would provide important new constraints for modeling the changes occurring in the Schiff base during the first two steps in the photocycle.

Does the X Intermediate Exist? Because of the existence of distinct bands at both 1539 and 1551 cm^{-1} in the photostationary spectrum of BR (cf. Figure 2), it is possible that two distinct intermediates are formed which under the conditions of these measurements would have to be in less than 17 μs. On the basis of the linear correlation between wavelength and stretching frequency, these bands would correspond to intermediates with wavelengths at 550 (1539 cm^{-1}) and 480 nm (1551 cm^{-1}) as previously suggested (Marcus & Lewis, 1978). The predicted 550-nm intermediate can be accounted for by L550 which is observed by kinetic absorption spectroscopy to form with a rise time of 2 μs (Stoeckenius et al., 1979). However, a second intermediate absorbing near 480 nm on the same time scale has not been observed in the BR photocycle. It is possible that X is a photoproduct of one of the early photocycle intermediates. However, the fact that the 1539- and 1551-cm^{-1} bands occur in fixed proportion to each other over a wide range of laser power for both 514.5- and 488.0-nm excitation tends to make this explanation unlikely.[6] A second possibility is that X exists in thermal equilibrium with L550. This might account for the absence of an X band in the low-temperature spectrum of L550 (Narva et al., 1981). However, this still does not explain the lack of evidence for X from visible absorption spectroscopy at room temperature. A third possibility is that the two bands at 1539 and 1551 cm^{-1} arise from a single intermediate L550. A splitting of C=C stretching vibrations is not completely unprecedented since it is observed in the resonance Raman spectrum of 3-dehydroretinal (Cookingham et al., 1978) and in the infrared spectrum of *all-trans*-retinal (Curry et al., 1982). It is possible that in L550, several double bonds with different stretching frequencies are strongly enhanced. Such a possibility might be tested by examining the L550 spectrum of isotopically labeled chromophores of BR as has been applied recently in the case of the K and M412 intermediates (Braiman & Mathies, 1980, 1982).

In conclusion, we have demonstrated that a combination of curve fitting and utilization of a spinning cell can be used to quantitatively extracts information about the early intermediates in the PM photocycle. Such an approach can also be used in conjunction with other kinetic methods such as a rapid flow system, eliminating the necessity for arbitrary weighting factors used in subtraction procedures. Our results confirm that L550 contains a protonated Schiff base and raise the possibility that the hypothesized X intermediate may reflect splitting in the ethylenic band of L550. Furthermore, the deprotonation of the bacteriorhodopsin Schiff base occurs at the L550 to M412 transition. There is some indication however, that a change in the local environment of the Schiff base proton occurs both during the bR570 to K step and the K to L550 step which is consistent with the existence of a proton switching mechanism.

Acknowledgments

We thank Dr. Virginia Culbertson, Kenneth M. Rosen, and Bill Cantore for excellent technical assistance, James Taaffe for building the photoelectric feedback system, and Dr. Lee Roberts for the program to compute the error function.

References

Argade, P. V. (1982) Ph.D. Thesis, Boston University.

Argade, P. V., & Rothschild, K. J. (1982) *Methods Enzymol. 88*, 643–648.

Argade, P. V., Rothschild, K. J., Kawamoto, A. H., Herzfeld, J., & Herlihy, W. C. (1981) *Proc. Natl. Acad. Sci. U.S.A. 78*, 1643–1646.

Armstrong, B. H. (1967) *J. Quant. Spectrosc. Radiat. Transfer 7*, 61–88.

Aton, B., Doukas, A. G., Callender, R. H., Becher, B., & Ebrey, T. G. (1977) *Biochemistry 16*, 2995–2999.

Becher, B. M., & Cassim, J. Y. (1975) *Prep. Biochem. 5*, 161–178.

Bevington, P. R. (1969) in *Data Reduction and Error Analysis for the Physical Sciences*, pp 134–246, McGraw-Hill, New York.

Braiman, M., & Mathies, R. (1980) *Biochemistry 19*, 5421–5428.

Braiman, M., & Mathies, R. (1982) *Proc. Natl. Acad. Sci. U.S.A. 79*, 403–407.

Callender, R. H., Doukas, A., Crouch, R., & Nakanishi, K. (1976) *Biochemistry 15*, 1621–1629.

Campion, A., El-Sayed, M. A., & Terner, J. (1977) *Biophys. J. 20*, 369–375.

Cookingham, R. E., Lewis, A., & Lemlye, A. T. (1978) *Biochemistry 17*, 5699.

Curry, B., Broek, A., Lugtenburg, J., & Mathies, R. (1982) *J. Am. Chem. Soc. 104*, 5274–5286.

[6] Hurley et al. (1978) reported that L′ is a photoproduct of L550, is photoreversible to L550, and can thermally relax to bR570. Furthermore, L′ has an absorption spectrum very similar to that of L550, but with a 3-nm shift and a 5% increase in intensity. Thus, if the 1551-cm^{-1} band originates from L′, then L′ would not follow the linear relation between λ_{max} and $\nu_{C=C}$.

Doukas, A. G., Aton, B., Callender, R. H., & Ebrey, T. G. (1978) *Biochemistry 17*, 2430-2435.
Engelman, D. M., Henderson, R., McLachlany, A. D., & Wallace, B. A. (1980) *Proc. Natl. Acad. Sci. U.S.A. 77*, 2023-2027.
Henderson, R., & Unwin, P. N. T. (1975) *Nature (London) 257*, 28-32.
Heyde, M. E., Gill, D., Kilponen, R. G., & Rimai, L. (1971) *J. Am. Chem. Soc. 93*, 6776-6780.
Hurley, J. B., Becher, B., & Ebrey, T. G. (1978) *Nature (London) 272*, 87-88.
Khorana, H. G., Gerber, G. E., Herlihy, W. C., Gray, C. P., Anderegg, R. J., Nihei, K., & Briemann, K. (1979) *Proc. Natl. Acad. Sci. U.S.A. 76*, 5040-5050.
Lewis, A., Spoonhower, J., Bogomolni, R. A., Lozier, R. H., & Stoeckenius, W. (1974) *Proc. Natl. Acad. Sci. U.S.A. 71*, 4462-4466.
Marcus, M. A., & Lewis, A. (1977) *Science (Washington, D.C.) 195*, 1328-1330.
Marcus, M. A., & Lewis, A. (1978) *Biochemistry 17*, 4722-4735.
Mathies, R., Oseroff, A. R., & Stryer, L. (1976) *Proc. Natl. Acad. Sci. U.S.A. 73*, 1-5.
Narva, D. L., Callender, R. H., & Ebrey, T. G. (1981) *Photochem. Photobiol. 33*, 567-571.
Ovchinnikov, Yu. A., Abdulaev, N. G., Fligina, M. Yu., Kiselev, A. V., & Lobanev, N. A. (1979) *FEBS Lett. 100*, 219-224.
Rimai, L., Kilponen, R. G., & Gill, D. (1970) *J. Am. Chem. Soc. 92*, 3824-3828.
Rothschild, K. J., & Marrero, H. (1982) *Proc. Natl. Acad. Sci. U.S.A. 79*, 4045-4049.
Rothschild, K. J., Argade, P. V., Earnest, T. N., Huang, K. S., London, E., Liao, M. J., Bayley, H., Khorana, H. G., & Herzfeld, J. (1982) *J. Biol. Chem. 257*, 8592-8595.
Sindius, T. (1973) *J. Raman Spectrosc. 1*, 471-488.
Stockburger, M., Klusmann, W., Gattermann, H., Massig, G., & Peters, R. (1979) *Biochemistry 18*, 4886-4900.
Stoeckenius, W., Lozier, R. H., & Bogomolni, R. A. (1979) *Biochim. Biophys. Acta 505*, 215-278.
Terner, J., & El-Sayed, M. A. (1978) *Biophys. J. 24*, 262-264.
Terner, J., Campion, A., & El-Sayed, M. A. (1977) *Proc. Natl. Acad. Sci. U.S.A. 74*, 5212-5216.
Terner, J., Hsieh, C., & El-Sayed, M. A. (1979a) *Biophys. J. 26*, 527-541.
Terner, J., Hsieh, C., Burns, A. R., & El-Sayed, M. A. (1979b) *Biochemistry 18*, 3629-3634.
Terner, J., Hsieh, C., Burns, A. R., & El-Sayed, M. A. (1979c) *Proc. Natl. Acad. Sci. U.S.A. 76*, 3046-3050.
Tsuda, M., Glaccum, M., Mellson, B., & Ebrey, T. G. (1980) *Nature (London) 287*, 351-353.

Structural Studies on the Membrane-Bound Immunoglobulin E-Receptor Complex. 1. Characterization of Large Plasma Membrane Vesicles from Rat Basophilic Leukemia Cells and Insertion of Amphipathic Fluorescent Probes†

David Holowka and Barbara Baird*

ABSTRACT: In order to investigate the properties of the membrane-bound IgE-receptor complex, a simple procedure has been adapted for preparing large plasma membrane vesicles from rat basophilic leukemia cells. These vesicles pinch off from the adherent cells after treatment with 2 mM *N*-ethylmaleimide or 50 mM formaldehyde and 1 mM dithiothreitol, and they are isolated from the supernatant after two centrifugation steps with yields of 20-25% of the initial cell-bound ^{125}I-IgE. With phase and fluorescence microscopy, micron-size vesicles are seen which are unilamellar and spherically shaped and devoid of intracellular organelles. On dextran gradients at least 70% of the ^{125}I-IgE is bound to membranes which band at low density, indicating large, intact vesicles that are impermeable to macromolecules. Between 60 and 75% of the bound ^{125}I-IgE is accessible to the external medium, showing the vesicles to be predominately right side out. This preparation was found to be suitable for resonance energy-transfer measurements. We have determined that amphipathic, fluorescent donor and acceptor probes partition into the vesicle bilayer in a randomly distributed, noninteracting manner. The densities of the probes can be ascertained directly from the amount of energy transfer that is observed as a function of acceptor concentration. This experimental system will allow energy-transfer measurements to determine distances between sites on receptor-bound IgE and the membrane surface.

Molecular details of the three-dimensional structure of mammalian cell surface receptor proteins are virtually unknown beyond basic information such as subunit composition and molecular weights. In particular little is known about the structure of receptors which bind immunoglobulins to mediate endocytosis or antigen-triggered transmembrane signaling (Unkless et al., 1981; Metzger et al., 1982). The receptor for immunoglobulin E (IgE)[1] may be the best characterized

† From the Department of Chemistry, Baker Laboratory, Cornell University, Ithaca, New York 14853. *Received December 28, 1982.* This work was supported by research grants from the American Chemical Society (PRF 12717), Research Corporation (Cottrell Grant), and the National Institutes of Health (AI18306).

[1] Abbreviations: IgE, immunoglobulin E; RBL, rat basophilic leukemia; HAF, 5-(hexadecanoylamino)fluorescein; HAE, 5-(hexadecanoylamino)eosin; HHC, 3-hexadecanoyl-7-hydroxycoumarin; ORB, octadecylrhodamine B chloride; FITC, fluorescein 5-isothiocyanate; $DiOC_n$-(3), 3,3′-dialkyloxacarbocyanine; NEM, *N*-ethylmaleimide; HCHO, formaldehyde; DTT, dithiothreitol; Hepes, *N*-(2-hydroxyethyl)piperazine-*N*′-2-ethanesulfonic acid; PBS, phosphate-buffered saline; $NaDodSO_4$, sodium dodecyl sulfate.

0006-2960/83/0422-3466$01.50/0